

Projected shell model study on nuclei near the $N = Z$ line

Yang Sun^a

Department of Physics, University of Notre Dame, Notre Dame, IN 46556, USA

Received: date / Revised version: date

Abstract. Study of the $N \approx Z$ nuclei in the mass-80 region is not only interesting due to the existence of abundant nuclear structure phenomena, but also important in understanding the nucleosynthesis in the rp-process. It is not feasible to apply a conventional shell model due to the necessary involvement of the $g_{9/2}$ sub-shell. In this paper, the projected shell model is introduced to this study. Calculations are systematically performed for the collective levels as well as the quasi-particle excitations. It is demonstrated that calculations with this truncation scheme can achieve a comparable quality as the large-scale shell model diagonalizations for ^{48}Cr , but the present method can be applied to much heavier mass regions. While the known experimental data of the yrast bands in the $N \approx Z$ nuclei (from Se to Ru) are reasonably described, the present calculations predict the existence of K -isomeric states, some of which lie low in energy under certain structure conditions.

PACS. 21.60.-n Nuclear-structure models and methods

1 Introduction

The proton-rich nuclei with particle number around 80 exhibit phenomena that are unique to this mass region. Unlike most heavy nuclei that have a stable deformation, the structure changes are quite pronounced among the neighboring nuclei, and this mass region is often characterized by shape co-existence. In addition, for $N \approx Z$ nuclei, there is an open question: Whether the neutron-proton correlations play an important role in the structure analysis. Finally, low-lying K -isomeric states can exist in the $Z \sim 34$ nuclei at an oblate minimum, and in the $Z \sim 44$ nuclei at a prolate one.

The study of these proton-rich nuclei is not only interesting from the nuclear structure point of view, but also has important implications in nuclear astrophysics. Since heavy elements are made in stellar evolution and explosions, nuclear physics, and in particular nuclear structure far from stability, enters into the stellar modelling in a crucial way. It is believed that these proton-rich nuclei near the $N = Z$ line are synthesised in the rapid-proton capture process (the rp-process) under appropriate astrophysical conditions, resulting in the creation of nuclei far beyond ^{56}Ni all the way to the proton rich regions of the chart of nuclides [1, 2]. The X-ray burst is suggested as a possible site. However, the nucleosynthesis and the correlated energy generation is not completely understood. In addition to the uncertainty of the astrophysical conditions, network simulations of the rp-process are hindered by the lack of experimental information on the structure of nuclei along

the rp-process path [1]. Nuclei of particular interest to the rp-process are the $N = Z$ waiting point nuclei [1].

Most of the nuclei in the mass-80 region are strongly deformed. At the deformed potential minimum, the high- j $g_{9/2}$ orbital intrudes into the pf-shell near the Fermi levels. Therefore, the $g_{9/2}$ orbitals dominate the low-lying structure of these nuclei, and these orbitals have to be included in the model space. A direct inclusion of the $g_{9/2}$ sub-shell into a conventional shell model calculation is not feasible. This strongly suggests a proper construction of a shell model basis that is capable of describing the undergoing physics within a manageable space.

The projected shell model (PSM) [3] is a shell model that builds its model space in a deformed basis. Unlike a conventional shell model that starts from a spherical basis, the PSM uses a deformed basis to start with. In this way, a large model space can be easily included and many nuclear correlations are already constructed before a configuration mixing is carried out. This makes shell model calculations for a heavy system possible. In the long history of the shell model development along this line, there have been different types of approaches (see, for example, Refs. [3, 4, 5, 6, 7]). Although these methods differ very much in details in the way of building the shell model bases and/or choosing effective interactions, they share the common characteristic that the model space is first constructed by physical guidance. The final diagonalization can therefore be carried out in a highly compact space, with each of the bases being a complicated combination in terms of the conventional shell model basis states.

The present paper applies the PSM to the study of proton-rich nuclei in the mass-80 region. We shall first demonstrate through the example of the ^{48}Cr calculation

^a e-mail: ysun@nd.edu

that the highly truncated calculations performed by the PSM can in fact achieve a comparable quality as the large-scale shell model diagonalizations. However, the present method can certainly be applied for much heavier mass regions. Based on the successful reproduction of the known experimental data of the yrast bands in the $N \approx Z$ nuclei (from Se to Ru), the present calculations further predict the existence of K -isomeric states, some of which lie low in energy under certain structure conditions. These low-energy isomers could have significant effects in the nucleosynthesis along the rp-process path.

2 The Projected shell model

2.1 Outline of the model

In a PSM calculation, the shell-model truncation is first achieved within the quasi-particle (qp) states with respect to the deformed Nilsson+BCS vacuum $|\phi\rangle$; then rotational symmetry (and number conservation if necessary) are restored for these states by standard projection techniques [8] to form a spherical basis in the laboratory frame; finally the shell model Hamiltonian is diagonalized in this basis. If one is mainly interested in the collective rotation with qp excitation, the truncation obtained in this way is very efficient. Usually, quite satisfactory results can be obtained by a diagonalization within a dimension smaller than 100. Clearly, such an approach lies conceptually between the two extreme methods [9]: deformed mean-field theories and conventional shell model, and thus can take the advantages of both.

The central technical question in this regard is how to compute the matrix elements in the projected states. Following the pioneering work of Hara and Iwasaki [10], a systematic derivation has been obtained for any one- and two-body operators (of separable forces) with an arbitrary number of quasi-particles in the projected states [3,11]. In principle, the projected multi-qp basis recovers the full shell model space if all the quasi-particles in the valence space are considered in building the multi-qp states. However, the advantage of working with a deformed basis is that the selection of only a few quasi-particles near the Fermi surface is already sufficient to construct a good shell model space. The rest can be simply truncated out.

The set of multi-qp states relevant to the present study (of even-even systems) is

$$|\Phi_\kappa\rangle = \{|0\rangle, a_{\nu_1}^\dagger a_{\nu_2}^\dagger |0\rangle, a_{\pi_1}^\dagger a_{\pi_2}^\dagger |0\rangle, a_{\nu_1}^\dagger a_{\nu_2}^\dagger a_{\pi_1}^\dagger a_{\pi_2}^\dagger |0\rangle\}, \quad (1)$$

where a^\dagger 's are the qp creation operators, ν 's (π 's) denote the neutron (proton) Nilsson quantum numbers which run over the low-lying orbitals, and $|0\rangle$ the Nilsson+BCS vacuum (or 0-qp state). Since the axial symmetry is kept for the Nilsson states, K is a good quantum number. It can be used to label the basis states in Eq. (1).

As in the usual PSM calculations, we use the Hamiltonian of separable forces [3]

$$\hat{H} = \hat{H}_0 - \frac{1}{2}\chi \sum_\mu \hat{Q}_\mu^\dagger \hat{Q}_\mu - G_M \hat{P}^\dagger \hat{P} - G_Q \sum_\mu \hat{P}_\mu^\dagger \hat{P}_\mu, \quad (2)$$

where \hat{H}_0 is the spherical single-particle Hamiltonian which in particular contains a proper spin-orbit force, whose strengths (i.e. the Nilsson parameters κ and μ) are taken from Ref. [12]. The second term in the Hamiltonian is the quadrupole-quadrupole (Q-Q) interaction and the last two terms, the monopole and quadrupole pairing interactions, respectively. Residual neutron-proton interactions are present only in the Q-Q term. It was shown [13] that these interactions simulate the essence of the most important correlations in nuclei, so that even the realistic force has to contain at least these components implicitly in order to work successfully in the structure calculations. As long as the physics under consideration is mainly of the quadrupole-and-pairing-type collectivities, we find no compelling reasons for not using these simple interactions. The interaction strengths are determined as follows: the Q-Q interaction strength χ is adjusted by the self-consistent relation such that the input quadrupole deformation ε_2 and the one resulting from the HFB procedure coincide with each other [3]. The monopole pairing strength G_M is taken to be $G_M = [G_1 - G_2(N - Z)/A]/A$ for neutrons and $G_M = G_1/A$ for protons, which was first introduced in Ref. [14]. The choice of the strengths G_1 and G_2 depends on the size of the single-particle space in the calculation. Finally, the quadrupole pairing strength G_Q is assumed to be proportional to G_M , the proportionality constant is usually taken in the range of 0.16 – 0.20.

The eigenvalue equation of the PSM for a given spin I takes the form

$$\sum_{\kappa'} \{H_{\kappa\kappa'}^I - E^I N_{\kappa\kappa'}^I\} F_{\kappa'}^I = 0, \quad (3)$$

where the Hamiltonian and norm matrix elements are respectively defined by

$$H_{\kappa\kappa'}^I = \langle \Phi_\kappa | \hat{H} \hat{P}_{KK'}^I | \Phi_{\kappa'} \rangle, \quad N_{\kappa\kappa'}^I = \langle \Phi_\kappa | \hat{P}_{KK'}^I | \Phi_{\kappa'} \rangle, \quad (4)$$

and \hat{P}_{MK}^I is the angular momentum projection operator [8]. The expectation values of the Hamiltonian with respect to a ‘‘rotational band κ ’’ $H_{\kappa\kappa}^I/N_{\kappa\kappa}^I$ are called the band energies. When they are plotted as functions of spin I , we call it a band diagram [3]. It usually provides us a useful tool for interpreting results.

2.2 An example: ^{48}Cr

^{48}Cr is a light nucleus for which an exact shell model diagonalization is feasible, yet exhibits remarkable high-spin phenomena usually observed in heavy nuclei: large deformation, typical rotational spectrum and the backbending in which the regular rotational band is disturbed by a sudden irregularity at a certain spin. This nucleus is therefore an excellent example for theoretical studies, providing a unique testing ground for various approaches [9,15].

In the PSM calculations for ^{48}Cr , three major shells ($N = 1, 2, 3$) are used for both neutron and proton. The strengths of the monopole pairing forces are chosen as $G_1 = 22.5$ and $G_2 = 18.0$ [14]. The quadrupole pairing

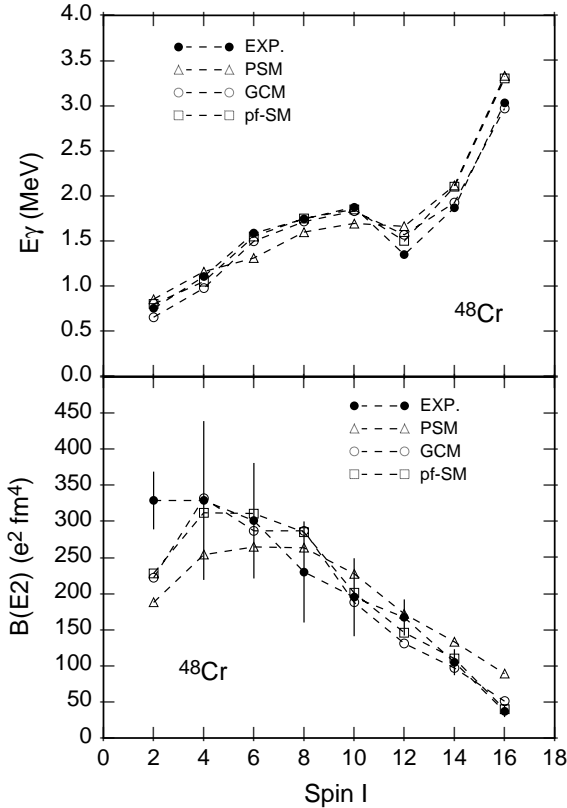


Fig. 1. Top panel: The γ -ray transition energies $E_\gamma = E(I) - E(I-2)$ as functions of spin. Bottom panel: The $B(E2)$ values as functions of spin. The experimental data are taken from Ref. [16] and the result of pf-SM from Ref. [9]. The PSM and GCM results are taken from Ref. [15].

strength G_Q is fixed as $0.2G_M$. The shell model space is truncated at the deformation $\varepsilon_2 = 0.25$.

In the top panel of Fig. 1, the results of the PSM for the γ -ray energy along the yrast band, together with that of the pf-shell model (pf-SM) reported in Ref. [9] and that of the Generator Coordinate Method (GCM) [15], are compared with the experimental data [16]. One sees that the four curves are bunched together over the entire spin region, indicating an excellent agreement of the three calculations with each other, and with the data. The sudden drop in E_γ occurring around spin 10 and 12 corresponds to the backbending in the yrast band of ^{48}Cr .

In the bottom panel of Fig. 1, the three theoretical results for $B(E2)$ are compared with the data [16]. All the three calculations use the same effective charges (0.5e for neutrons and 1.5e for protons). Again, one sees that the theoretical descriptions agree not only with each other but also with the data quite well. The $B(E2)$ values decrease monotonously after spin 6 (where the first band crossing takes place in the PSM). This implies a monotonous decrease of the intrinsic Q-moment as a function of spin, reaching finally the spherical regime at higher spins. This implies also that the final results of shell model calculations do not depend on the choice of the single-particle

states (spherical or deformed) in building a shell model space.

Fig. 1 indicates that the PSM is a reasonable shell model truncation scheme as it reproduces the result of the large-scale pf-SM very well. Furthermore, the advantage of the PSM is that it is able to extract the underlying physics. Here, it is to understand why and how the backbending occurs. A band diagram displays band energies of various configurations before they are mixed by the diagonalization procedure Eq.(3). Irregularity in a spectrum may appear if a band is crossed by another one at certain spin. It was found [15] that in ^{48}Cr , the backbending is caused by a band crossing that corresponds to a simultaneous alignment of the $f_{7/2}$ neutron and proton pairs.

Following the success in the ^{48}Cr calculation, it has been demonstrated in Ref. [17] that the PSM can, using the same set of parameters as used for ^{48}Cr , describe the odd-mass nuclei $^{47,49}\text{V}$, $^{47,49}\text{Cr}$ and $^{49,51}\text{Mn}$, which have also been extensively studied with the large-scale pf-SM diagonalizations [18]. Another recent PSM work [19] has shown that the model can be applied to the odd-odd nuclei near the $N = Z$ line as well.

3 The $N \approx Z$ nuclei in the mass-80 region

3.1 Properties of the yrast bands

In $N = Z$ nuclei, neutrons and protons occupy the same orbitals, and thus can have the largest probability to interact with each other. The study of $N = Z$ nuclei is the domain which is expected to give the most relevant information about the properties of the neutron-proton (n-p) interaction. An interesting question for the yrast band properties is whether the expected strong n-p interaction will modify the rotational-alignment picture in $N = Z$ nuclei. It has been suggested using the cranking approaches in a single- j shell (see the references cited in Ref. [20]) that the rotational-alignment properties can be modified by the residual n-p interaction. The recently observed alignment delays in ^{72}Kr , ^{76}Sr , and ^{80}Zr [21] were conjectured as possible consequences of the strong n-p pairing interaction.

Experimentally locating the band crossings in these $N \approx Z$ nuclei is a very challenging task. The main difficulty in extending the study of $N = Z$ nuclei to high spins is that their population has extremely low cross sections in the small number of available reactions. Despite of the difficulties, progress in the development of large γ -ray arrays and associated ancillary detectors, and refinements of the data processing techniques, has allowed recent advance in the knowledge of some heavier $N = Z$ nuclei (see, for example, Refs. [21,22,23,24]).

Parallel to the experimental efforts, a systematic investigation for the yrast properties of the $N = Z$, $Z+2$, and $Z+4$ in Kr, Sr and Zr nuclei has been carried out by the PSM [25]. The calculations described reasonably well most of the observables (moments of inertia, transition quadrupole moments and g-factors) known for these nuclei, with a notable exception: the very pronounced delay in the crossing frequency in ^{72}Kr [21]. To understand

Table 1. Deformations ε_2 at which the projected bases are constructed for the nuclei presented in Fig. 2.

$N = Z$ nuclei	ε_2	$N = Z+2$ nuclei	ε_2
^{72}Kr	0.36	^{74}Kr	0.36
^{76}Sr	0.36	^{78}Sr	0.36
^{80}Zr	0.36	^{82}Zr	0.29
^{84}Mo	0.28	^{86}Mo	0.22
^{88}Ru	0.23	^{90}Ru	0.16

this disagreement, a more detailed PSM analysis for the $N = Z$ Kr, Sr and Zr nuclei was subsequently performed [20]. While inclusion of an empirically enhanced residual n-p interaction in the Q-Q channel was found helpful to improve the agreement with the data, it was realized also that this enhancement offsets the good agreement previously obtained for the $N \neq Z$ nuclei $^{74,76}\text{Kr}$ with the standard interaction strength [20] (see Fig. 2 below).

Very recently, the observation of another band in ^{72}Kr has been reported [24], which solved our puzzle why the ^{72}Kr rotational-alignment should exhibit such an unusual behavior as suggested in Ref. [21]. Calculations show that this new band could be the missing aligned S-band, which lies much closer to what was predicted [25].

To show to what extent the yrast properties of these nuclei can be understood by the PSM in a systematical way, we have calculated the $N = Z$ and $N = Z+2$ isotopes from $Z = 36$ to 44. The calculations are performed by using three major shells ($N = 2, 3, 4$) for both neutrons and protons, with the pairing interaction strengths $G_1 = 20.25$ and $G_2 = 16.20$, and the quadrupole-pairing constant $G_Q = 0.16G_M$, for all the nuclei considered (These strengths are the same as those used in Ref. [25]). Table 1 lists the deformation parameters, at which the shell model spaces are constructed. The results are presented in Fig. 2.

As can be seen, the standard PSM calculations describe quite well the moments of inertia of the $N = Z+2$ nuclei up to the highest measured spin. In particular, the fine structure at the band crossing regions is quantitatively reproduced. The calculations also predict well the known data for the $N = Z$ nuclei in this region. Going from lighter to heavier nuclei along the $N = Z$ line, one finds that the degree of band disturbance varies, exhibiting back-bend (Kr), no bend (Sr), slight up-bend (Zr), up-bend (Mo), back-bend (Ru). The PSM analysis suggests that this systematical behavior in band disturbance may be analogous to what has been known in the rare-earth region [26]. From Kr to Ru isotopes, the closest orbitals to the Fermi levels move gradually from $K = 1/2$ and $3/2$ to $K = 5/2$ and $7/2$ states of the $g_{9/2}$ shell. Since the crossing bands are the 2-qp states having components from the near-Fermi orbitals, different shell fillings make the effective band interactions at the crossing region rather different, resulting in different disturbances in the yrast bands.

However, it is still an open question whether the standard set of the PSM interactions is sufficient to describe the yrast properties of these $N = Z$ nuclei. The present

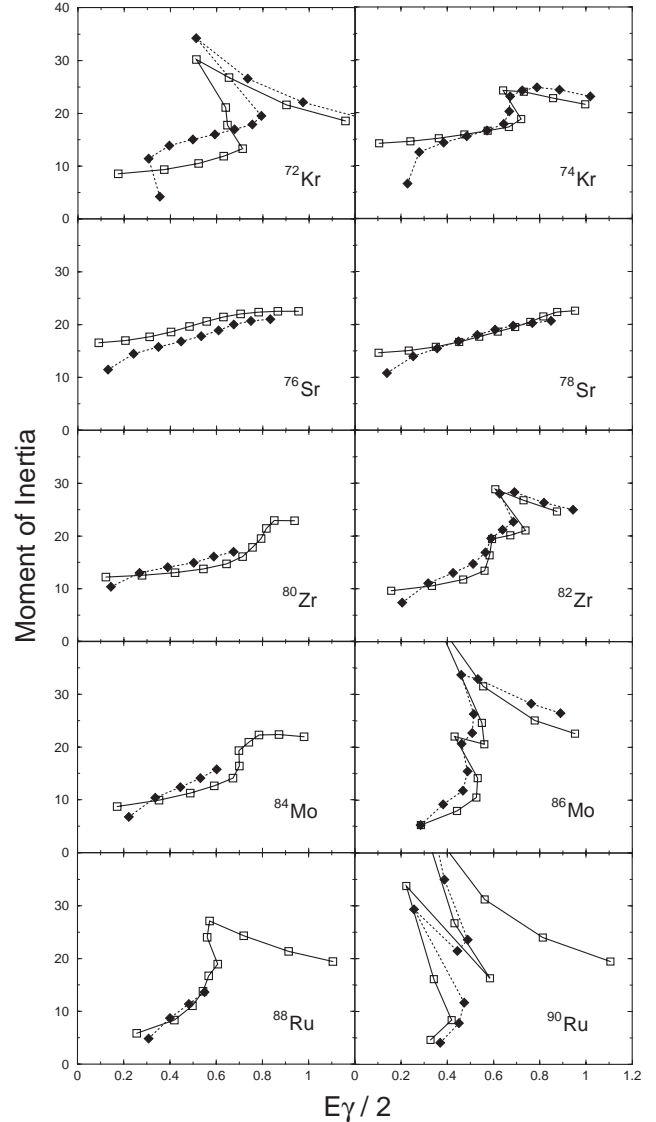


Fig. 2. Comparison of the calculated yrast energy levels with known data for $N = Z$ and $N = Z + 2$ nuclei in the plots of moment of inertia $\mathfrak{I}^{(1)}(I) = (2I - 1)/E_\gamma(I \rightarrow I - 2)$ vs. rotational frequency $\omega(I) = E_\gamma(I \rightarrow I - 2)/2$.

data for ^{80}Zr [21], ^{84}Mo [22], and ^{88}Ru [23] stop just before the spin states where band disturbances are predicted to occur. The PSM calculations with an empirically enhanced n-p interaction (results not shown) suggested higher alignment frequencies [22]. Thus, although the existing experimental data seem to indicate some delays of the alignment frequency in comparison with the neighboring $N = Z + 2$ nuclei, one cannot immediately relate this to an enhancement of the n-p interaction. From Fig. 2 one may only conclude that at least two or three more yrast transitions are very much desired in these $N = Z$ nuclei for a better testing of the PSM predictions.

3.2 K -isomeric states

In an axially-deformed system, K is a good quantum number. Conservation of K leads to selection rules for transitions involving changes in K between the initial and final states, which in turn lead to decay hindrances resulting in isomers. Depending on the degree of the transition hindrance, some high- K isomeric states can be very long-lived [27]. Long-lived isomers are not only interesting from the structure point of view, they may also be found important in the interdisciplinary fields. For nuclear astrophysics, information regarding the structure of isomeric states and the nearby states is very valuable. One recent example [28, 29] is the study of the excitation and decay of $^{180}\text{Ta}^m$ in understanding the nuclear astrophysics puzzle on the production and survival of ^{180}Ta in stars.

It has been argued that the existence of isomers in nuclei along the rp-process path could significantly modify the current conclusions on the nucleosynthesis and the correlated energy generation in X-ray bursts [1]. Along the $N = Z$ line, there are waiting point nuclei whose lifetimes entirely determine the speed of nucleosynthesis towards heavier nuclei and the produced isotopic abundances. The lifetimes are strongly dependent on the photodisintegration rates, the β -decay rates, and particularly on the masses of nuclei along the path. If there are isomeric states in the low-energy region in these nuclei, the total β -decay half-life of an isotope, for example, can be affected strongly if an isomeric state is populated and has a significantly different β -decay half-life compared to the ground state. Therefore, knowing the existence and the structure of the isomers could have a significant impact.

Shape co-existence phenomenon has been observed in the mass-80 region. There is evidence that at $Z \sim 34$ the oblate shape can be energetically favored, while for heavier nuclei (with $Z \sim 44$) the prolate shape dominates. It is interesting to realize that near the $N \approx Z$ line, in both deformed energy minima (oblate for $Z \sim 34$ and prolate for $Z \sim 44$ systems), the K -components of the $g_{9/2}$ sub-shell are found to be high. Among the nuclei discussed in this paper, the $K = 7/2$ and $9/2$ orbitals lie close to the Fermi levels in the Se isotopes at oblate deformations, and the $K = 5/2$ and $7/2$ orbitals are found near the Fermi levels in the Zr, Mo, and Ru isotopes at their prolate minima. Quasi-particles of these orbitals can couple to a $K = 8$ 2-qp state in the former, and a $K = 6$ 2-qp state in the latter case.

In Table 2, the predicted energy levels of the $I^\pi = 6^+$ isomeric states (relative to the ground state) in the $N = Z$ and $N = Z + 2$ Zr, Mo, and Ru isotopes are given. Our prediction is based on realistic calculations that have reasonably reproduced all the known structure data in these nuclei (see Fig. 2). To indicate how high these states lie above the yrast band, energies of the $I^\pi = 6^+$ levels in the ground band are also shown. It is worth pointing out that the same K -components that couple to a $K = 6$ 2-qp state can give rise to a crossing band if they couple to a $K = 1$ 2-qp state, causing the band disturbances as discussed in Fig. 2.

Table 2. The predicted energy levels of $I^\pi = 6^+$ isomeric state (relative to the ground state) in $N = Z$ and $N = Z + 2$ nuclei. The calculated $I^\pi = 6^+$ levels in the ground band are also shown.

Nuclei	$E(I^\pi = 6^+_{\text{ground}})$ (MeV)	$E(I^\pi = 6^+_{\text{isomer}})$ (MeV)
^{80}Zr	1.65	4.19
^{82}Zr	1.91	3.71
^{84}Mo	2.03	3.53
^{86}Mo	2.51	3.21
^{88}Ru	2.35	3.14
^{90}Ru	2.17	2.38

3.3 Structure of the waiting-point nucleus ^{68}Se

The predicted shape coexistence in ^{68}Se seems to be firmly suggested by the recent experimental data [30]. Two co-existing rotational bands were identified, with the ground state band having properties consistent with collective oblate rotation, and the excited band having characteristics consistent with prolate rotation. Our PSM calculations are performed for ^{68}Se at deformation $\varepsilon_2 = 0.28$ for the prolate states, and $\varepsilon_2 = -0.24$ for the oblate states. The calculation conditions are the same as used for the nuclei in Fig. 2, except for slightly reduced pairing strengths: $G_1 = 19.58$ and $G_2 = 15.66$. In addition, we found that the recently suggested Nilsson parameter set [31] works better for the description of ^{68}Se .

Fig. 3 compares the results of ^{68}Se for the lowest levels of each spin, and at the prolate and oblate minima. Good agreement has been obtained for the known oblate band. The calculations suggest a gradual increase in the moment of inertia extended to higher spin states beyond the current experimental band [30]. In contrast, the moment of inertia of the prolate band behaves rather differently. The data bend back sharply as the rotational frequency increases. This basic feature in the prolate band has also been reproduced by the calculation. In addition to the observed sharp backbending at spin 8, we predict a second sharp backbending at spin 16.

At the prolate minimum in ^{68}Se , the Fermi levels are surrounded by the low- K states, whereas at the oblate minimum, they are near the high- K states. The low- and high- K states respond rather differently to the rotation, which is reflected in very different rotational alignments. Detailed analysis [32] using the band diagrams suggested that the $K = 1$ band based on $g_{9/2}$ quasiparticles with $K = 7/2$ and $9/2$ at the oblate minimum crosses the 0-qp band so gently that one cannot see a band disturbance in the yrast solution. However, the $K = 1$ band based on $g_{9/2}$ quasiparticles with $K = 1/2$ and $3/2$ at the prolate minimum crosses the 0-qp band sharply. In the latter case, the regular band is disturbed, resulting in the observed first bankbending. The predicted second backbending is caused by a crossing of the 4-qp band that consists of a proton and a neutron pair [32].

In the same calculation, we predict high- K bands ($K = 8$) with a bandhead of spin 8 and an excitation energy of 5 MeV. They are long-lived isomeric states in the sense

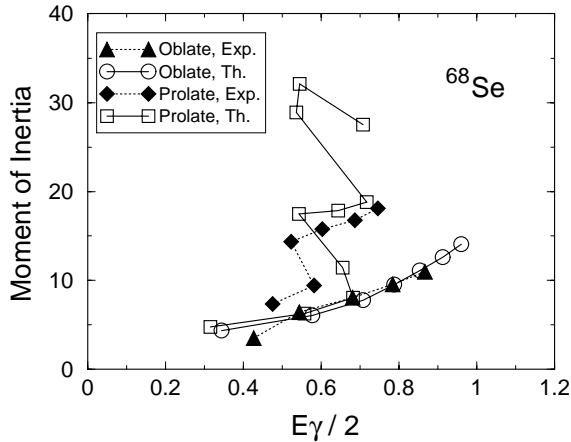


Fig. 3. Comparison of the calculated yrast energy levels with known data in ^{68}Se in the plot of Moments of inertia $\mathfrak{S}^{(1)}(I) = (2I-1)/E_\gamma(I \rightarrow I-2)$ vs. rotational frequency $\omega(I) = E_\gamma(I \rightarrow I-2)/2$. The experimental data are taken from Ref. [30].

that no allowed γ -transition matrix elements of low multipolarity can connect these states to the nearby ground band ($K = 0$). Thus, once the isomeric states are populated, the high- K states find no path for further γ -decay. An analysis with inclusion of the isomeric states in the rp-process network simulations is in progress [33].

4 Summary

One of the frontiers in nuclear physics is the study of nuclei far from the β -stability. It is desired to apply advanced shell model diagonalization methods while pushing the calculations to heavy nuclear systems. However, most of the spherical shell model calculations are severely limited in the fp-shell nuclei or nuclei in the vicinity of shell closures.

We have shown that the projected shell model may be an efficient truncation scheme of the exact shell model solution. In the calculation for ^{48}Cr , the PSM results are comparable with those obtained by the large-scale shell model calculations. Systematic calculations are performed for the collective levels as well as the quasi-particle excitations for the $N \approx Z$ nuclei in the mass-80 region. While the known experimental data of the yrast bands (from Se to Ru) are quantitatively described, the present calculations predict the existence of K -isomeric states, some of which lie low in energy under certain structure conditions. We hope that these states can be identified experimentally. It will be highly interesting to see how much their presence modifies the current conclusions of the rp-process nucleosynthesis.

The author wishes to express his sincere thanks to D. Bucurescu and C.A. Ur for motivating him to study this interesting mass region. Valuable discussions with J.A. Sheikh and C.J. Lister, as well as with A.V. Afanasjev, A. Aprahamian, S. Frauendorf, and M. Wiescher are acknowledged. This work is supported by the NSF under contract number PHY-0140324.

References

1. H. Schatz, *et al.*, Phys. Rep. **294** (1998) 167.
2. H. Schatz, *et al.*, Phys. Rev. Lett. **86** (2001) 3471.
3. K. Hara and Y. Sun, Int. J. Mod. Phys. **E4** (1995) 637.
4. K.W. Schmid and F. Grümmer, Rep. Prog. Phys. **50**, 731 (1987).
5. C.-L. Wu, D. H. Feng and M. Guidry, Adv. Nucl. Phys. **21** (1994) 227.
6. G. Popa, J.G. Hirsch and J.P. Draayer, Phys. Rev. **C62** (2000) 064313.
7. T. Otsuka, Nucl. Phys. **A704** (2002) 21c.
8. P. Ring and P. Schuck, *The Nuclear Many Body Problem* (Springer-Verlag, New York, 1980).
9. E. Caurier, *et al.*, Phys. Rev. Lett. **75** (1995) 2466.
10. K. Hara and S. Iwasaki, Nucl. Phys. **A332** (1979) 61; **A348** (1980) 200.
11. Y. Sun and K. Hara, Comput. Phys. Comm. **104** (1997) 245.
12. T. Bengtsson and I. Ragnarsson, Nucl. Phys. **A436** (1985) 14.
13. M. Dufour and A.P. Zuker, Phys. Rev. **C54** (1996) 1641.
14. W. Dieterich, *et al.*, Nucl. Phys. **A253** (1975) 429.
15. K. Hara, Y. Sun and T. Mizusaki, Phys. Rev. Lett. **83** (1999) 1922.
16. F. Brandolini, *et al.*, Nucl. Phys. **A642** (1998) 387.
17. V. Velázquez, J.G. Hirsch and Y. Sun, Nucl. Phys. **A686** (2001) 129.
18. G. Martínez-Pinedo, A.P. Zuker, A. Poves and E. Caurier, Phys. Rev. **C55** (1997) 187.
19. R. Palit, J.A. Sheikh, Y. Sun, and H.C. Jain, Phys. Rev. **C67** (2003) 014321.
20. Y. Sun and J.A. Sheikh, Phys. Rev. **C64** (2001) 031302(R).
21. S.M. Fischer, *et al.*, Phys. Rev. Lett. **87** (2001) 132501.
22. N. Mărginean, *et al.*, Phys. Rev. **C65** (2002) 051303(R).
23. N. Mărginean, *et al.*, Phys. Rev. **C63** (2001) 031303(R).
24. N.S. Kelsall, *et al.*, Proceedings of the Conference on Frontiers of Nuclear Structure, Berkeley, USA, Jul. 29 - Aug. 2, 2002.
25. R. Palit, J.A. Sheikh, Y. Sun, and H.C. Jain, Nucl. Phys. **A686** (2001) 141.
26. R. Bengtsson, I. Hamamoto and B.R. Mottelson, Phys. Lett. **73B** (1978) 259.
27. P. Walker and G. Dracoulis, Nature (London) **399** (1999) 35.
28. D. Belic, *et al.*, Phys. Rev. Lett. **83** (1999) 5242; Phys. Rev. **C65** (2002) 035801.
29. P.M. Walker, G.D. Dracoulis and J.J. Carroll, Phys. Rev. **C64** (2001) 061302(R).
30. S.M. Fischer, *et al.*, Phys. Rev. Lett. **84** (2000) 4064.
31. Y. Sun, *et al.*, Phys. Rev. **C62** (2000) 021601(R).
32. Y. Sun, Z.-W. Ma, A. Aprahamian and M. Wiescher, nucl-th/0107004.
33. A. Aprahamian and M. Wiescher, private communication.